Identification of a Covalent Importin-5 Inhibitor, Goyazensolide, from a Collective Synthesis of Furanoheliangolides

Liu, Weilong; Patouret, Rémi; Barluenga Badiola, Sofia; Plank, Michaël; Loewith, Robbie Joséph; Winssinger, Nicolas

How to cite

LIU, Weilong et al. Identification of a Covalent Importin-5 Inhibitor, Goyazensolide, from a Collective Synthesis of Furanoheliangolides. In: ACS Central Science, 2021, vol. 7, n° 6, p. 954–962. doi: 10.1021/acscentsci.1c00056

This publication URL: https://archive-ouverte.unige.ch/unige:152644
Publication DOI: 10.1021/acscentsci.1c00056

ACS central science

http://pubs.acs.org/journal/acscii

Research Article

Identification of a Covalent Importin-5 Inhibitor, Goyazensolide, from a Collective Synthesis of Furanoheliangolides

Weilong Liu,[#] Rémi Patouret,[#] Sofia Barluenga, Michael Plank, Robbie Loewith, and Nicolas Winssinger*

Cite This: *ACS Cent. Sci.* 2021, 7, 954–962

Read Online

ACCESS | Metrics & More | Article Recommendations | Supporting Information

ABSTRACT: Sesquiterpenes are a rich source of covalent inhibitors with a long history in traditional medicine and include several important therapeutics and tool compounds. Herein, we report the total synthesis of 16 sesquiterpene lactones via a build/couple/pair strategy, including goyasensolide. Using an alkyne-tagged cellular probe and proteomics analysis, we discovered that goyazensolide selectively targets the oncoprotein importin-5 (IPO5) for covalent engagement. We further demonstrate that goyazensolide inhibits the translocation of RASAL-2, a cargo of IPO5, into the nucleus and perturbs the binding between IPO5 and two specific viral nuclear localization sequences.

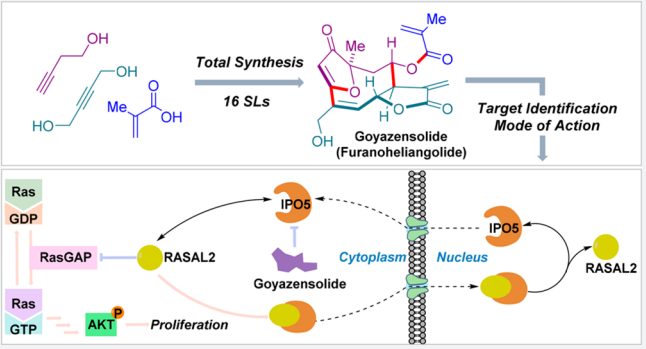

INTRODUCTION

Goyazensolide (**1**, Figure 1), a member of the furanoheliangolide sesquiterpene family, has been isolated from several plants used in traditional medicine and was first identified in a screen for schistosomicidal agents.[1] It has also been shown to be effective in an animal model bearing a colon tumor (HT-29 xenograft)[2] and as a potential treatment for neurofibromatosis type 2 (NF2),[3] for which there is currently no FDA-approved intervention. There is clear evidence that goyazensolide inhibits the expression of genes under the control of *c-myb*, a proto-oncogenic transcription factor;[4] however, its exact mode of action remains undefined. 15-Deoxygoyazensolide (**3**, Figure 1) was found to be slightly more cytotoxic than goyazensolide,[5] suggesting that small modifications can enhance activity. 15-Deoxygoyazensolide was also found to be active in a number of quantitative-cell-based reporter assays.[6]

The activity of sesquiterpenes often hinges on the presence of Michael acceptors that can engage a target covalently.[7,8] A well-studied example is helenalin, used therapeutically as an anti-inflammatory, which inhibits the NF-κB pathway by covalent interaction with cysteines in p65, thereby precluding the interaction of p65 with DNA.[9] Another example is ainsliadimer A, which was shown to selectively inhibit IKK kinase by reaction with Cys46 present in an allosteric pocket.[10] Our own studies on deoxyelephantopin led to the discovery that it reacts with PPAR-γ and antagonizes the function of this nuclear receptor by engaging a cysteine located in the zinc-finger motif.[11]

While some sesquiterpenes are readily available from natural sources, understanding the covalent interactome requires the synthesis of probes that cannot always be achieved by direct functionalization of the natural product and requires a total synthesis.

RESULT AND DISCUSSION

Collective Synthesis of Furanoheliangolides. Furanoheliangolides are secondary metabolites produced from farnesyl pyrophosphate by cyclization, involving the germacrenyl cation intermediate and subsequent oxidative reactions (Figure 1a).[12] The promiscuity of this biosynthetic pathway yields a range of closely related analogues akin to combinatorial library synthesis.[13] The collective synthesis of furanoheliangolides and related natural products (**1**–**17**, Figures 1 and S1), including goyazensolide (**1**), was envisioned via a gold-catalyzed transannulation of key intermediates **18** to generate the strained bicyclic framework (Figure 1b).[14] Disconnection of the C7–C8 and C3–C4 bonds (Barbier-type allylation and Sonogashira coupling, respectively) would reduce the complexity to readily available synthons (**20**–**23**) amenable to a build/couple/pair strategy.[15,16]

Received: January 13, 2021
Published: May 25, 2021

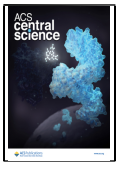

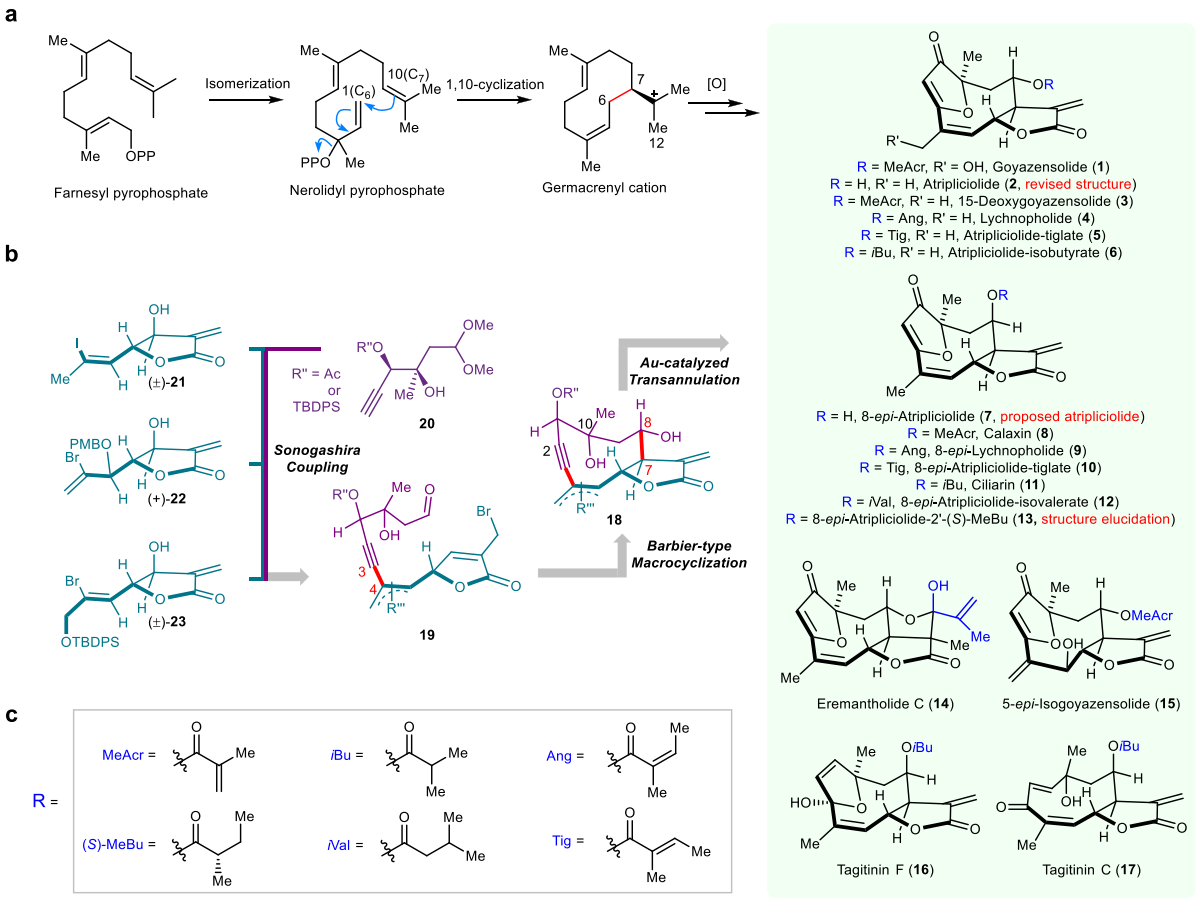

Figure 1. Biosynthesis and retrosynthetic analysis for the collective synthesis of furanoheliangolides through a build/couple/pair strategy. (a) Schematic biosynthesis of furanoheliangolides and related sesquiterpene (**1**−**17**) from farnesyl pyrophosphate. (b) Retrosynthetic analysis for the collective synthesis of **1**−**17**. (c) Structure of the different side chains (R).

In the synthetic direction, key intermediate **20a** (Scheme 1) was obtained in five steps from vinyl alcohol **24** via a sequence involving a one-pot Dess−Martin periodinane (DMP) oxidation, acetal protection followed by a Sonogashira coupling with trimethylsilylacetylene (**24** → **25**), Sharpless asymmetric dihydroxylation (SAD) of the enyne,[17] selective secondary alcohol protection (**25** → **26**), and desilylation of the acetylene.[18] The sequence delivers the intermediate **20a** with 39% overall yield and 91% *ee* on a decagram scale. The second intermediate **21** was prepared in two steps from aldehyde **27** and allyl bromide **28** by Barbier allylation/lactonization (**27** + **28** → **29**) followed by SeO_2 allylic oxidation (**29** → **21**). While asymmetric synthesis of this synthon is possible, we used a racemic product with an interest for both diastereomers resulting in the pairing of alkyne **20a** and vinyl iodide **21**.

Sonogashira coupling (**20a** + **21**, reaction A) followed by PBr_3 (reaction B) to convert the allylic alcohol in a bromide (S_N2') with concomitant deprotection of the dimethyl acetal afforded the cyclization precursor **19a**. Treatment of **19a** with $CrCl_2$ (reaction C) in DMF afforded a clean transformation to the desired germacrene framework as a separable mixture of the two diastereomers (**18a** and **30**) arising from the undefined stereocenter at C6. While nuclear Overhauser effect (NOE) patterns clearly discerned the two diastereoisomers, the structure of **30** was confirmed by X-ray diffraction (CCDC2049428, Supplementary Section m). The strained 10-member ring of the germacrene framework is challenging to synthesize, and to the best of our knowledge, this is the first example merging the α-methylene-γ-butyrolactone formation with the closure of a 10-membered germacrene framework. Further diversification to the furanoheliangolide proved to be highly efficient following the removal of the silyl protecting group (**18a** → **31**, reaction D). Selective oxidation of the propargyl alcohol (MnO_2) followed by treatment with tBu$_3$PAuNTf$_2$ (reaction E) afforded the furanoheliangolide **2**.

It is noteworthy that the spectral data of **2** matched the reported data of atripliciolide.[19] The stereochemical assignment was further validated by X-ray analysis (CCDC2049427, Supplementary Section m). Analysis of other possible diastereoisomers on route to **32** or **7** did not match the NMR data, thus allowing a revision of the structure of atripliciolide as **2** (Supplementary Section c). Acylation of the unique hydroxyl group of atripliciolide with the different possible side chains (reaction F) afforded 15-deoxygoyazensolide (**3**) and related natural products **4**−**6** (Supplementary Section e). 15-Deoxygoyazensolide (**3**) was further converted to eremantholide C (**14**) using Stryker's reagent.[20] The reaction sequence (D−F) to convert the germacrene framework to furanoheliangolide was also used to convert **30** into a hitherto unreported 15-deoxygoyazensolide diastereoisomer **32**.

Based on a number of furanoheliangolides having an *R*-stereochemistry at C8, we sought to invert the stereochemistry of the hydroxyl at this position in intermediate **18a** (Scheme

https://doi.org/10.1021/acscentsci.1c00056
ACS Cent. Sci. 2021, 7, 954−962

Scheme 1. Diversification of Germacrene Framework and Synthesis of Furanoheliangolides

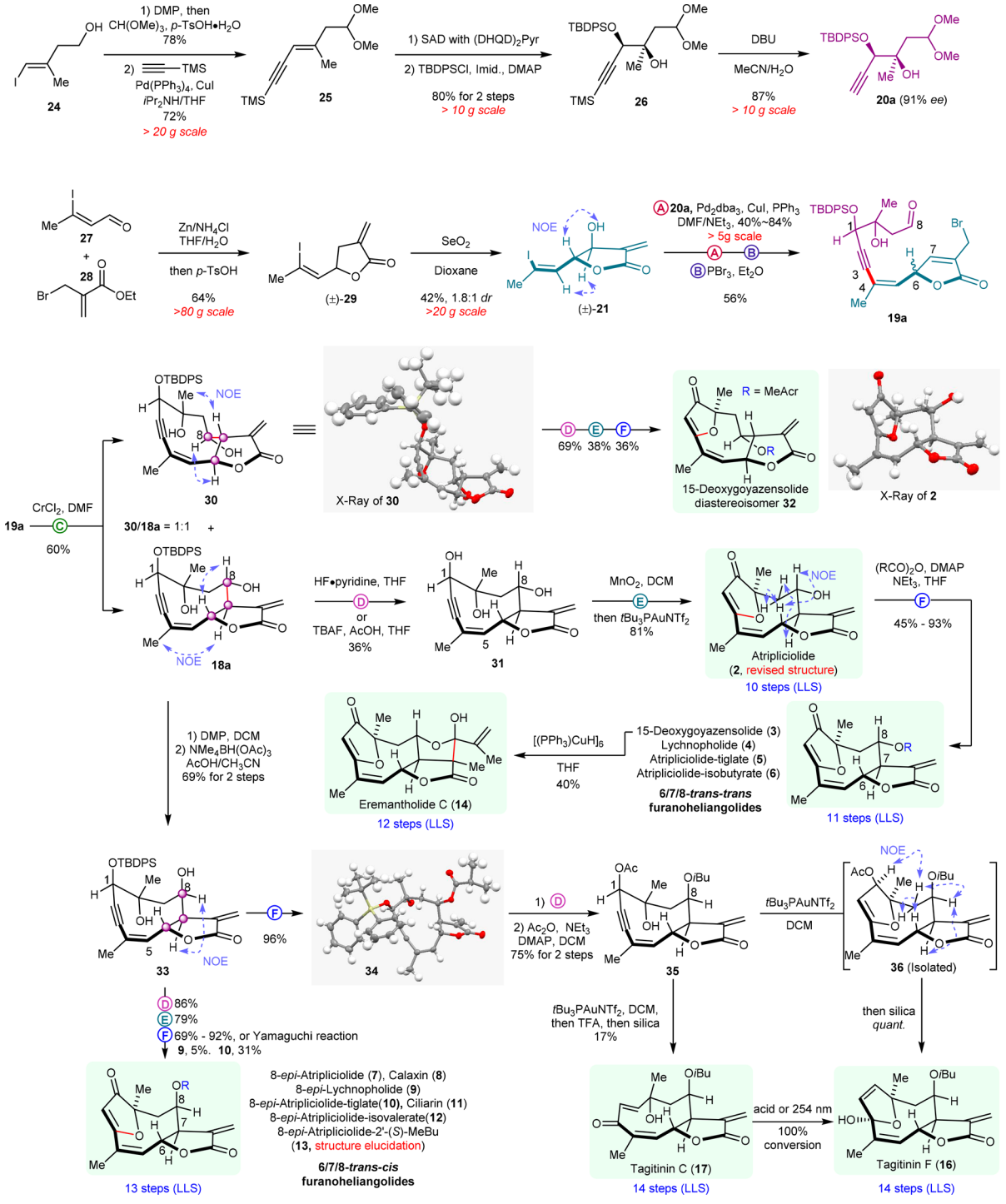

1). The most efficient protocol proved to be a DMP oxidation followed by an Evans−Saksena reduction[21] leveraged on the chelation of the C10 hydroxyl, to afford **33** as a single diasteroisomer. The stereochemical assignment was verified by X-ray diffraction of the acylated intermediate **34** (CCDC2049429, Supplementary Section m). Applying the reaction sequence (D−F) to convert this germacrene framework (**33**) to furanoheliangolides afforded six new natural products (**8**−**13**, Supplementary Section e). These syntheses also allowed the stereochemistry to be established in the side chain of 8-*epi*-atriplociolide-2′-(*S*)-MeBu,[22] which remained undefine hitherto. Comparison of other diasteroisomers provided an unequivocal match (Supplementary Section d).

Germacrene **34** was used to access yet another set of natural products employing a slight modification in the reaction sequence (Scheme 1): acetylation of the C1 hydroxyl (**35**) rather than oxidation to a propargyl ketone as in the previous sequence. While we anticipated that **35** could be converted to tagitinin C (**17**) using the gold catalysis ($tBu_3PAuNTf_2$) directly via a Meyer−Schuster rearrangement,[23] we obtained tagitinin F (**16**) instead. However, using the same catalyst in DCM followed by a TFA treatment did yield tagitinin C (**17**),

https://doi.org/10.1021/acscentsci.1c00056
ACS Cent. Sci. 2021, 7, 954−962

albeit in low yield due to its instability (**17** → **16**).[24] The synthetic **16** and **17** were identical to authentic samples (Supplementary Section e). This insight came from analysis of the reaction pathway by NMR (Figure S7). Based on the observed reaction intermediates, we propose that the mechanism (Figure S8) proceeds by a gold activation of the alkyne to yield intermediate **36**. This intermediate then undergoes a [3,3]-sigmatropic rearrangement followed by a hydrolysis to afford tagitinin F (**16**). Given sufficiently acidic conditions, the acetal can open to facilitate the *Z*- to *E*- olefin isomerization, thus yielding tagitinin C (**17**).

Exploiting the same synthetic sequence with a different pairing strategy afforded 5-*epi*-isogoyazensolide (**15**) and goyazensolide (**1**) as shown in Scheme 2. 5-*epi*-Isogoyazensolide (**15**) comes from the pairing of **22** with **20a** (propargylic hydroxyl protected with *tert*-butyldiphenylsilyl), whereas goyazensolide comes from the pairing of **23** with **20b** (propargylic hydroxyl protected with an acetate). Synthon **22** was prepared from 1,4-pentadien-3-ol (**37**) in five steps by a known protocol[25] (asymmetric center introduced by Sharpless asymmetric dihydroxylation) followed by a diastereoselective allylic oxidation (SeO_2). Synthon **23** was prepared following the same sequence as for **21** from known alcohol **38**.

Scheme 2. Further Pairing and Stereoselective Synthesis of 5-*epi*-Isogoyazensolide (15), Goyazensolide (1), and Probes GOYA-1 and GOYA-2

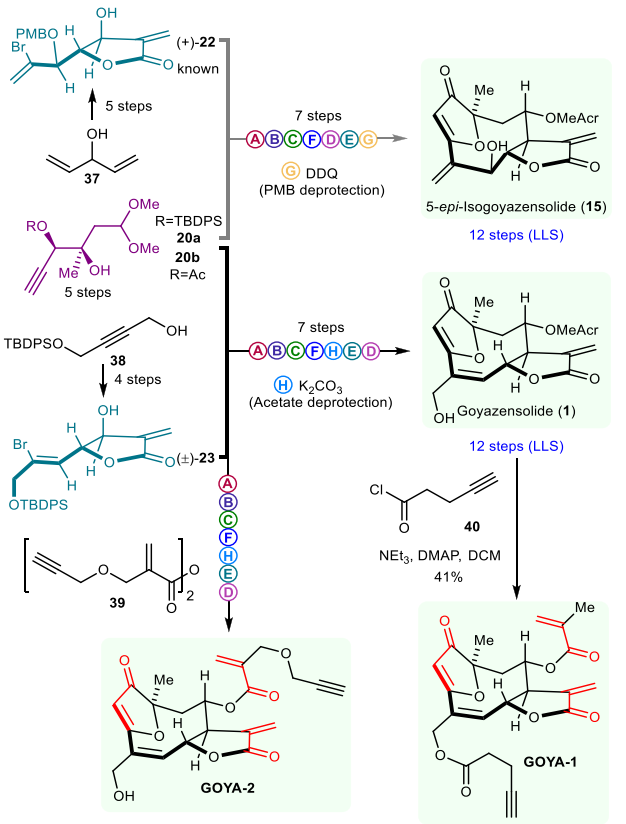

It is important to note that the pairing of **22** and **20a** yields a single diastereoisomer affording **15** enantioselectively. In both cases, the spectroscopic data fully matched that of the natural isolate (Supplementary Section e). These syntheses also enabled the preparation of goyazensolide probes tagged with an alkyne group (**GOYA-1** and **GOYA-2**) for subsequent labeling studies.

Thus, this simple build/couple/pair sequence afforded germacrene frameworks (**18a**, **30**, **33**, etc.), which can be further diversified into 16 natural products (**1**−**6**, **8**−**17**) within 10−14 steps, none of which had been previously synthesized.

Goyazensolide Interacts Covalently with Importin-5 (IPO5). The presence of multiple Michael acceptors in goyazensolide (**1**) and their similarity to those of other covalent inhibitors in the sesquiterpene lactone family led us to speculate that goyazensolide interaction with its target could be also covalent. Indeed, the *α-exo*-methylene-*γ*-butyrolactone moiety of goyazensolide is present in many sesquiterpenes (>1000), including helenalin (**H**, Figure 2e), and the disposition of this functionality with respect to the second Michael acceptor (methacrylate side chain) is precisely the same as in deoxyelephantopin (**D**, Figure 2e). The furanone endows goyazensolide with a third Michael acceptor. Having access to the natural product, we decided to synthesize a goyazensolide probe with the intention of preparing an activity-based probe for a proteome-wide target screen (Figure 2a).[26,27] With this in mind, we first acylated the primary allylic alcohol with 4-pentynoyl chloride (**40** → **GOYA-1**, Scheme 2), as had been previously done successfully for helenalin derivatives.[28] To our surprise, alkyne-tagged **GOYA-1** did not afford meaningful protein labeling in a crude extract (30 min of labeling, CuAAC coupling with **Cy3**−$\mathbf{N_3}$ and SDS-PAGE analysis, Figure 2b, left). Increasing the probe concentration and reaction time did not improve the results.

We thus explored another position to introduce the alkyne and *de novo* synthesized **GOYA-2** (Scheme 2), with the alkyne extending from the methyl acrylate side chain. Treatment of crude lysate from PC3 cells with **GOYA-2** followed by reaction with **Cy3**−$\mathbf{N_3}$ and SDS-PAGE revealed a strong band at around 120 kDa that was specifically competed when the lysate had been previously treated with the unmodified goyazensolide (Figure 2b, right). Lysates from five other cancer cell lines (HeLa, K562, U2OS, HT-29, SW620) showed a similar profile, suggesting this target was not cell-line-specific (Figure S15). Competition with other sesquiterpenes (Figure 2e) containing the same *α-exo*-methylene-*γ*-butyrolactone (helenalin, lactucin), the similar unsaturated side chain (thapsigargin), or the combination of both (deoxyelephantopin, cnicin, cynaropicrin) showed that none of them competed for the same target as goyazensolide (Figure 2f).

In order to enrich the targeted proteins, we performed a pull-down using streptavidin beads of the cell lysate treated with **GOYA-2** after reaction with desthiobiotin−**Cy3**−$\mathbf{N_3}$ (Figure S13) and visualized the result on an SDS-PAGE. A triple in-gel digestion of the Cy3 band with trypsin/GluC/chemotrypsin and analysis of the sample by MS/MS afforded a list of peptides corresponding to proteins, which were filtered by molecular weight (between 105−145 kDa) and coverage (>15 unique peptides detected for each protein), resulting in four candidates (Figure 2c). The protein with highest coverage was IPO5 (63 unique peptides, 41% coverage) followed by pyruvate carboxylase (52 unique peptides, 33% coverage), UBA1 (19 unique peptides, 18% coverage), and ACLY (18 unique peptides, 13% coverage). The identity of the target was confirmed by a Western blot with an antibody specific for IPO5. The same experiment with anti-UBA1 antibody or anti-ACLY antibody did not yield signal above background (Figure

https://doi.org/10.1021/acscentsci.1c00056
ACS Cent. Sci. 2021, 7, 954−962

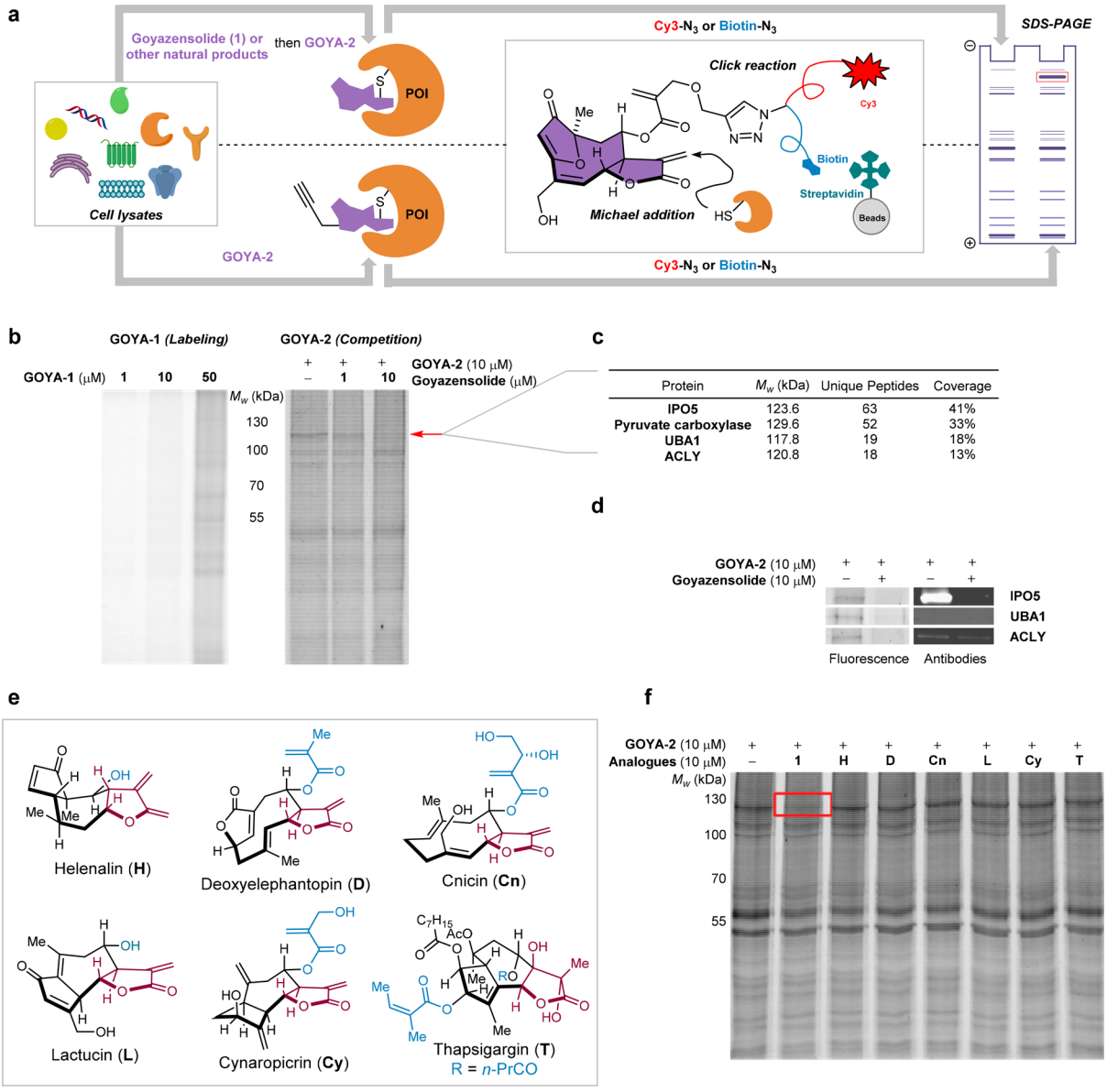

Figure 2. Target identification of goyazensolide with alkynylated probe **GOYA-2**. (a) Workflow schema for proteomic wide target identification, by competition and pull-down. POI, protein of interest. (b) Left, proteomic profile in PC3 cells using **GOYA-1** at 1, 10, or 50 μM for 30 min at room temperature (RT), followed by a CuAAC reaction with **Cy3−N$_3$** (cyanine 3-azide). Right, proteomic profile and competition with goyazensolide in PC3 cells using **GOYA-2** probe at 10 μM followed by reaction with **Cy3−N$_3$**. (c) Number of unique peptides and coverage of top four proteins identified based on enrichment in PC3 cell line. IPO5, importin 5; UBA1, ubiquitin-like modifier-activating enzyme 1; ACLY, ATP-citrate synthase. (d) Immunoblot of competitive pull-down upon treatment of PC3 cell lysate with DMSO or goyazensolide (10 μM, 30 min) followed by **GOYA-2** (10 μM, 30 min), CuAAC reaction with biotinylated fluorophore, and streptavidin enrichment. (e) Structures of other sesquiterpene lactones containing similar Michael acceptors used in the competition experiment. (f) SW620 lysate was incubated for 30 min with DMSO or one of the natural products (10 μM, 30 min) and then labeled with 10 μM **GOYA-2** followed by a CuAAC reaction with **Cy3−N$_3$** for 1 h at RT in the dark, and then, samples were analyzed by SDS-PAGE.

2d). Pyruvate carboxylase was enriched due to its endogenous biotinylation, and it was still detectable by MS/MS in the control experiment, employing unmodified goyazensolide as a competitor, whereas IPO5 was not (Figure S16).

IPO5 (also known as Ran-binding protein 5 (RANBP5) or karyopherin beta-3 (KPNB3)) is a member of the importin β family, a group of proteins which transport cargo to the nucleus. Further experiments indicated that goyazensolide was indeed a selective binder for IPO5 compared to other importins (Figure S17). While the function of IPO5 remains largely unstudied, it has been shown to be an interesting target for the treatment of tumors and viral infections (*vide infra*). To the best of our knowledge, no pharmacological modulators of IPO5 have been reported to date. We also extended the experiment by using **GOYA-2** in competition with the other natural products synthesized (Figures 3a and S18). The assay revealed that only atripliciolide (**2**) was as effective as goyazensolide, suggesting that the interaction of goyazensolide with IPO5 does not require the acrylate side chain at C8. However, the C8 stereochemistry seems to be critical for the binding (Figure 3a, e.g., **2** vs **7**).

Goyazensolide Inhibits the Interaction of IPO5 with Specific Nuclear Localization Sequences (NLSs). IPO5 has been shown to be recruited by influenza A to transport

https://doi.org/10.1021/acscentsci.1c00056
ACS Cent. Sci. 2021, 7, 954−962

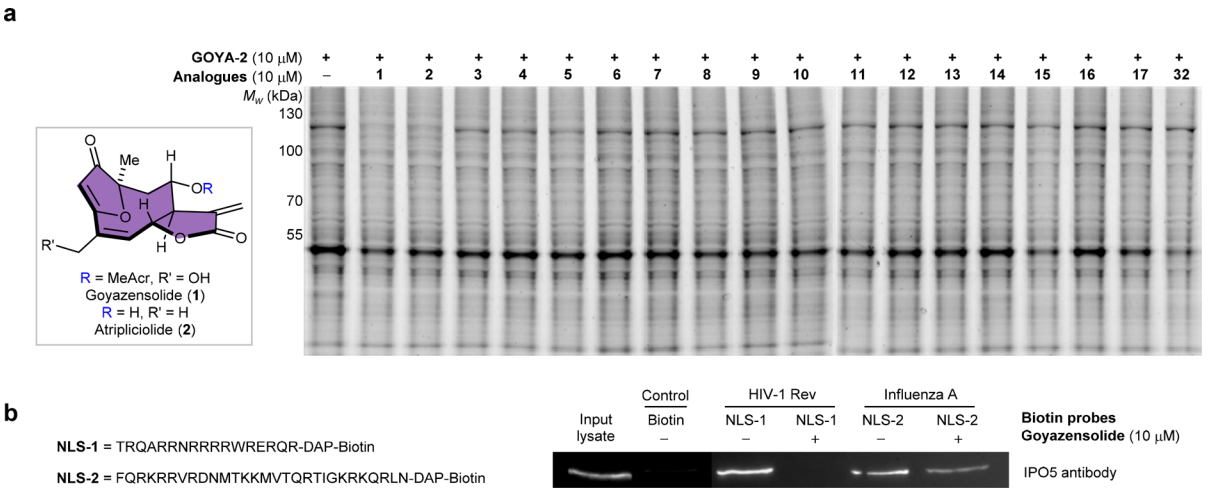

Figure 3. Competition experiments with the other natural products synthesized, and goyazensolide inhibits the interaction of IPO5 with specific NLSs. (a) SW620 lysate was incubated for 30 min with DMSO or one of the natural products (10 μM, 30 min) and then labeled with 10 μM **GOYA-2** followed by a CuAAC reaction with **Cy3−N_3** for 1 h at RT in the dark and analyzed by SDS-PAGE using fluorescence as a readout. The labeling/competition experiment shows selective binding of goyazensolide (**1**) and atripliciolide (**2**) to IPO5. (b) Left, sequence of two viral biotinyleted NLSs, **NLS-1** (HIV Rev) and **NLS-2** (PB1 influenza A). Right, immunoblot of competitive interaction between NLS and IPO5. Magnetic streptavidin beads were saturated with corresponding NLSs and then incubated for 2 h with HT29 lysate treated with DMSO or goyazensolide (10 μM, 30 min).

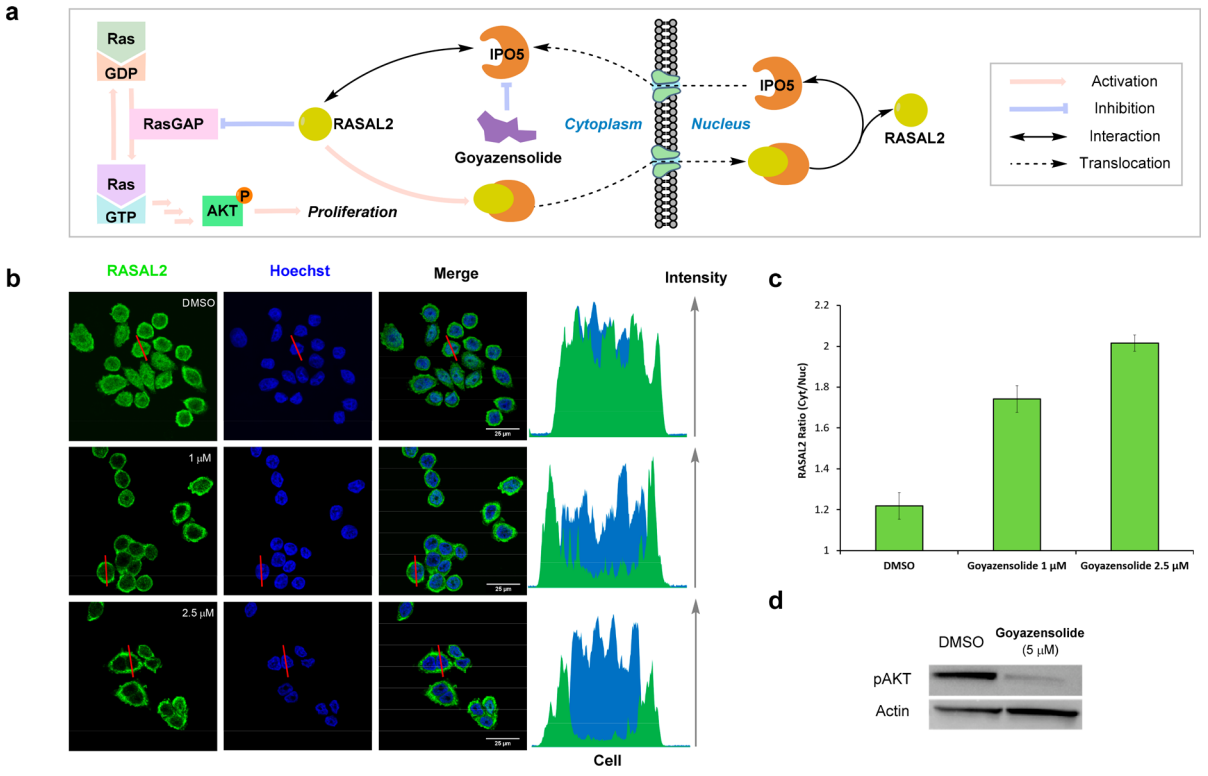

Figure 4. Covalent engagement of IPO5 with goyazensolide inhibits its transport activity in cells. (a) Illustration of IPO5 involvement in the Ras pathway. (b) Confocal microscopy images of SW620 cells treated with DMSO or 1 or 2.5 μM goyazensolide for 3 h, imaging of localization of RASAL2 using an RASAL2 primary antibody followed by an Alexa fluor488 secondary antibody (green), nuclear stain with Hoechst (blue), and fluorescence quantification of the images. Fluorescence intensity profile across the red line is shown on the right. (c) Ratio of fluorescence in cytosol versus nucleus (number of cells > 15). (d) Immunoblot of p-AKT (p-AKT Ser473 antibody) expression upon treatment of SW620 cells with DMSO or goyazensolide (5 μM, 4 h).

essential cargo to the nucleus, and disruption of the interaction between the NLS of the influenza A protein PB1 and IPO5 inhibits viral replication.[29] IPO5 is also important for the transport of viral proteins of HCV and HIV.[30] To test whether goyazensolide was effective at inhibiting the interaction between IPO5 and the NLSs of viral proteins, the sequences **NLS-1** (NLS of Rev; HIV) and **NLS-2** (NLS of PB1; influenza A) (Figures 3b and S20) were coupled to biotin tags and loaded on magnetic beads for pull-down experiments with IPO5. In the absence of an inhibitor, both NLS sequences

https://doi.org/10.1021/acscentsci.1c00056
ACS Cent. Sci. 2021, 7, 954−962

effectively pulled-down IPO5, as observed in a Western blot of the elution fraction (Figure 3b). Addition of goyazensolide (10 μM) to the cell lysates prior to the addition of the beads inhibited the pull-down of IPO5. Thus, the covalent interaction between goyazensolide and IPO5 inhibits its interaction with these two NLSs.

Goyazensolide Inhibits the Cellular Function of IPO5. IPO5 has been shown to be involved in the transport of RAS protein activator-like 2 (RASAL2) to the nucleus, a negative regulator of RasGAP. Thus, nuclear translocation of RASAL2 frees RasGAP to convert inactive Ras-GDP to active Ras-GTP as shown in Figure 4a.[31] The ratio of cytosolic RASAL2 and nuclear RASAL2 was clearly shown to depend on IPO5 using siRNA silencing of IPO5 (increased cytosolic concentration of RASAL2) and IPO5 overexpression (decreased cytosolic concentration of RASAL2).[31] In order to understand if goyazensolide could phenocopy the silencing activity of siRNA targeting IPO5, an SW620 colon cancer cell line was used to measure the RASAL2 ratio in the cytosol vs the nucleus in the presence and the absence of goyazensolide (Figure 4b). In the absence of treatment, the cytosolic/nuclear ratio of RASAL2 is 1.2. Upon treatment with 1.0 or 2.5 μM goyazensolide for 3 h, the ratio increased to 1.8 and 2.0, respectively (Figure 4c). Thus, goyazensolide treatment led to an increased cytosolic /nuclear ratio of RASAL2 in a dose dependent fashion.

Since the inhibition of RASAL2 translocation to the nucleus should have a downstream effect on the level of pAKT, we also monitored the level of pAKT (Ser473) in the presence or absence of drug. As shown in Figure 4d, treatment with 5 μM goyazensolide led to a dramatic reduction of pAKT. Collectively, these experiments demonstrate that IPO5 is the target of goyazensolide and that covalent engagement of IPO5 inhibits its transport activity *in cellulo*.

Sesquiterpenes are a rich source of bioactive compounds, and their syntheses continue to challenge synthetic chemists (for recent examples, see refs 32−35). From a synthetic chemistry perspective, goyazensolide stands out as a highly oxidized member of the germacranolides with protean C3 and C10 bridged furan ring featuring an anti-Bredt double bond. The present work demonstrates that despite its complexity, such natural products can now be accessed synthetically in less than 13 steps. The strategy employed is compatible with a build/couple/pair strategy facilitating the collective synthesis of multiple natural products, including goyazensolide. This required a cyclization to form a 10-membered ring, which is notoriously difficult. The use of Barbier allylation to simultaneously install the α-*exo*-methylene-γ-butyrolactone and achieve this cyclization is unprecedented in this context, and the work reported indicates that it is a robust strategy to access the strained framework. The use of an alkyne in the ring facilitates the pairing chemistry by mild and efficient Sonogashira coupling, and the alkyne offers divergent functionalization pathways to furanoheliangolide or related heliangolides. The chemistry described enabled the collective synthesis of 16 complex sesquiterpene lactones, many with important biological activity (See Figure S1 for a complete set of reference to biological activity).

The use of some of these compounds in traditional medicine gives them the benefit of a preliminary toxicology profile in humans. However, the lack of information on the mode of action often precludes a more insightful and targeted use of such compounds. In the case of goyazensolide, there was clear evidence of anticancer activity from mouse xenografts and cellular assays, but the mode of action remained unknown. The finding that goyazensolide selectively engages IPO5 covalently and inhibits its interaction with cargo rationalizes its anticancer activity and points to potential antiviral applications. IPO5 is highly expressed in colorectal cancer[31] and esophageal cancer.[36] As an antiviral target, there is clear evidence that IPO5 is recruited by viruses and that its trafficking activity is essential in the viral replication cycle.[29,30]

The fact that a small molecule can outcompete a high-affinity interaction with larger molecular entities such as the interaction of transportin with an NLS sequence of a protein underpins the unique features of covalent inhibitors. Transport of cargo between the cytoplasm and nucleus is a highly regulated process with the nuclear pore complex acting as a molecular sieve restricting diffusion. Translocation thus requires active transport leveraged on the action of a superfamily of karyopherin (importin and exportin).[37] The ability to modulate this traffic with small molecules is empowering,[38,39] but there are only few examples thus far. The first example of a small molecule regulating a karyopherin is leptomycin B, a polyketide bearing a Michael acceptor, which selectively inhibits exportin-1 (XPO-1, also known as chromosome region maintenance 1 (CRM1))[40] by reacting with its target.[41] This discovery led to significant medicinal chemistry efforts resulting in a molecule (selinexor) that is FDA-approved for multiple myeloma.[42]

The second example, ivermectin, was identified from a high-throughput screen for inhibitors of protein nuclear import. Characterization of the nuclear transport inhibitory properties of ivermectin demonstrated that it is a broad-spectrum inhibitor of importin α/β nuclear import with potent antiviral activity toward both HIV-1 and dengue virus, both of which are strongly reliant on importins.[43] Notably, this FDA-approved drug also inhibits SARS-CoV-2 replication. Studies on SARS-CoV proteins have revealed a potential role for importin α/β1 heteroduplex in nucleocytoplasmic shuttling of the SARS-CoV's nucleocapsid protein.[44] IPO5 has clearly been shown to be implicated in the transport of influenza A's RNA polymerase,[45] and mutations affecting binding to IPO5 severely attenuate viral growth,[29] suggesting this activity could be phenocopied with small molecule inhibitors of IPO5. The crystal structure of IPO5 coupled to docking studies of the NLS revealed critical interactions of influenza's PA−PB1 subcomplex with IPO5.[46]

CONCLUSION

In summary, we report the first total synthesis of goyazensolide and 15 related natural products. Our studies revise the stereochemical assignment of two natural products. Significantly, this synthesis enabled the study of the covalent interactome of goyazensolide, revealing IPO5 as its molecular target. The covalent engagement inhibits the interaction of IPO5 with cargos, provides a rationale for its cytotoxic activity in several cancer cell lines, and points to potential antiviral activity.

The resurging interest in covalent inhibitors brings renewed interest to sesquiterpenes, particularly those that have already been used in traditional medicine, affording a preliminary assessment of toxicity. Covalent inhibition is particularly attractive if target binding is in competition with strong endogenous interactions such as in protein−protein interactions or transcription factors interacting with DNA.

https://doi.org/10.1021/acscentsci.1c00056
ACS Cent. Sci. 2021, 7, 954−962

■ ASSOCIATED CONTENT

Supporting Information

The Supporting Information is available free of charge at https://pubs.acs.org/doi/10.1021/acscentsci.1c00056.

Additional figures and tables, experimental details for the synthesis of all new compounds including experimental procedures, characterization and spectral data, detailed information for biological materials, cell culture and preparation of lysates, pull-down experiments, in-gel tryptic digestion, LC−MS/MS analysis, mass spectrometry analysis, preparation of **NLS-1** and **NLS-2**, pull-down experiment with viruses' NLS, microscopy and data analysis, and pAKT assay (PDF)

■ AUTHOR INFORMATION

Corresponding Author

Nicolas Winssinger − *Department of Organic Chemistry, NCCR Chemical Biology, Faculty of Science, University of Geneva, 1211 Geneva, Switzerland;* orcid.org/0000-0003-1636-7766; Email: Nicolas.Winssinger@unige.ch

Authors

Weilong Liu − *Department of Organic Chemistry, NCCR Chemical Biology, Faculty of Science, University of Geneva, 1211 Geneva, Switzerland*

Rémi Patouret − *Department of Organic Chemistry, NCCR Chemical Biology, Faculty of Science, University of Geneva, 1211 Geneva, Switzerland*

Sofia Barluenga − *Department of Organic Chemistry, NCCR Chemical Biology, Faculty of Science, University of Geneva, 1211 Geneva, Switzerland*

Michael Plank − *Department of Molecular Biology, NCCR Chemical Biology, Faculty of Science, University of Geneva, 1205 Geneva, Switzerland*

Robbie Loewith − *Department of Molecular Biology, NCCR Chemical Biology, Faculty of Science, University of Geneva, 1205 Geneva, Switzerland*

Complete contact information is available at: https://pubs.acs.org/10.1021/acscentsci.1c00056

Author Contributions

#W.L. and R.P. contributed equally.

Notes

The authors declare no competing financial interest.

The raw data has been deposited on Zenodo (https://zenodo.org/record/4314704).

■ ACKNOWLEDGMENTS

We thank Céline Besnard for assistance with X-ray diffraction studies, Prof. Daniela Aparecida Chagas de Paula for authentic samples of tagitinin C/F, and Prof. Gil Valso Jose da Silva and Prof. Constantino for an authentic sample of goyazensolide. This work was supported by the Swiss National Science Foundation (188406) and NCCR Chemical Biology (185898).

■ REFERENCES

(1) Vichnewski, W.; Sarti, S. J.; Gilbert, B.; Herz, W. Goyazensolide, a Schistosomicidal Heliangolide from Eremanthus-Goyazensis. *Phytochemistry* **1976**, *15*, 191−193.

(2) Acuna, U. M.; Shen, Q.; Ren, Y.; Lantvit, D. D.; Wittwer, J. A.; Kinghorn, A. D.; Swanson, S. M.; Carcach de Blanco, E. J. Goyazensolide Induces Apoptosis in Cancer Cells in vitro and in vivo. *Int. J. Cancer Res.* **2013**, *9*, 36−53.

(3) Spear, S. A.; Burns, S. S.; Oblinger, J. L.; Ren, Y. L.; Pan, L.; Kinghorn, A. D.; Welling, D. B.; Chang, L. S. Natural Compounds as Potential Treatments of NF2-Deficient Schwannoma and Meningioma: Cucurbitacin D and Goyazensolide. *Otol. Neurotol.* **2013**, *34*, 1519−1527.

(4) Schomburg, C.; Schuehly, W.; Da Costa, F. B.; Klempnauer, K. H.; Schmidt, T. J. Natural sesquiterpene lactones as inhibitors of Myb-dependent gene expression: Structure-activity relationships. *Eur. J. Med. Chem.* **2013**, *63*, 313−320.

(5) Ren, Y. L.; Gallucci, J. C.; Li, X. X.; Chen, L. C.; Yu, J. H.; Kinghorn, A. D. Crystal Structures and Human Leukemia Cell Apoptosis Inducible Activities of Parthenolide Analogues Isolated from Piptocoma rufescens. *J. Nat. Prod.* **2018**, *81*, 554−561.

(6) Kearney, S. E.; Zahoranszky-Kohalmi, G.; Brimacombe, K. R.; Henderson, M. J.; Lynch, C.; Zhao, T. G.; Wan, K. K.; Itkin, Z.; Dillon, C.; Shen, M.; et al. Canvass: A Crowd-Sourced, Natural-Product Screening Library for Exploring Biological Space. *ACS Cent. Sci.* **2018**, *4*, 1727−1741.

(7) Ren, Y. L.; Yu, J. H.; Kinghorn, A. D. Development of Anticancer Agents from Plant-Derived Sesquiterpene Lactones. *Curr. Med. Chem.* **2016**, *23*, 2397−2420.

(8) Lagoutte, R.; Winssinger, N. Following the Lead from Nature with Covalent Inhibitors. *Chimia* **2017**, *71*, 703−711.

(9) Lyss, G.; Knorre, A.; Schmidt, T. J.; Pahl, H. L.; Merfort, I. The anti-inflammatory sesquiterpene lactone helenalin inhibits the transcription factor NF-kappa B by directly targeting p65. *J. Biol. Chem.* **1998**, *273*, 33508−33516.

(10) Dong, T.; Li, C.; Wang, X.; Dian, L. Y.; Zhang, X. G.; Li, L.; Chen, S.; Cao, R.; Li, L.; Huang, N.; et al. Ainsliadimer A selectively inhibits IKK alpha/beta by covalently binding a conserved cysteine. *Nat. Commun.* **2015**, *6*, 6522.

(11) Lagoutte, R.; Serba, C.; Abegg, D.; Hoch, D. G.; Adibekian, A.; Winssinger, N. Divergent synthesis and identification of the cellular targets of deoxyelephantopins. *Nat. Commun.* **2016**, *7*, 12470.

(12) Miller, D. J.; Allemann, R. K. Sesquiterpene synthases: passive catalysts or active players? *Nat. Prod. Rep.* **2012**, *29*, 60−71.

(13) Fischbach, M. A.; Clardy, J. One pathway, many products. *Nat. Chem. Biol.* **2007**, *3*, 353−355.

(14) Alcaide, B.; Almendros, P.; Alonso, J. M. Gold catalyzed oxycyclizations of alkynols and alkyndiols. *Org. Biomol. Chem.* **2011**, *9*, 4405−4416.

(15) Nielsen, T. E.; Schreiber, S. L. Diversity-oriented synthesis - Towards the optimal screening collection: A synthesis strategy. *Angew. Chem., Int. Ed.* **2008**, *47*, 48−56.

(16) Mortensen, K. T.; Osberger, T. J.; King, T. A.; Sore, H. F.; Spring, D. R. Strategies for the Diversity-Oriented Synthesis of Macrocycles. *Chem. Rev.* **2019**, *119*, 10288−10317.

(17) Brummond, K. M.; Lu, J. L.; Petersen, J. A rapid synthesis of hydroxymethylacylfulvene (HMAF) using the allenic Pauson-Khand reaction. A synthetic approach to either enantiomer of this illudane structure. *J. Am. Chem. Soc.* **2000**, *122*, 4915−4920.

(18) Yeom, C. E.; Kim, M. J.; Choi, W.; Kim, B. M. DBU-promoted facile, chemoselective cleavage of acetylenic TMS group. *Synlett* **2008**, *2008*, 565−568.

(19) Bohlmann, F.; Singh, P.; Zdero, C.; Ruhe, A.; King, R. M.; Robinson, H. Naturally-Occurring Terpene Derivatives 0.413. Furanoheliangolides from 2 Eremanthus Species and from Chresta-Sphaerocephala. *Phytochemistry* **1982**, *21*, 1669−1673.

(20) Sass, D. C.; Heleno, V. C. G.; Cavalcante, S.; da Silva Barbosa, J. D.; Soares, A. C. F.; Constantino, M. G. Solvent Effect in Reactions Using Stryker's Reagent. *J. Org. Chem.* **2012**, *77*, 9374−9378.

(21) Evans, D. A.; Chapman, K. T.; Carreira, E. M. Directed Reduction of Beta-Hydroxy Ketones Employing Tetramethylammonium Triacetoxyborohydride. *J. Am. Chem. Soc.* **1988**, *110*, 3560−3578.

(22) Bohlmann, F.; Dutta, L. N. Naturally Occurring Terpene Derivatives 0.184. New Heliangolide from Helianthus-Lehmannii. *Phytochemistry* **1979**, *18*, 676−676.
(23) Engel, D. A.; Dudley, G. B. The Meyer-Schuster rearrangement for the synthesis of alpha,beta-unsaturated carbonyl compounds. *Org. Biomol. Chem.* **2009**, *7*, 4149−58.
(24) Fernandes, V. H. C.; Viera, N. D.; Zanini, L. B. L.; Silva, A. D.; Salem, P. P. D.; Soare, M. G.; Nicacio, K. D.; de Paula, A. C. C.; Virtuoso, L. S.; Oliveira, T. B.; et al. Efficient Method to Obtain Tagitinin F by Photocyclization of Tagitinin C. *Photochem. Photobiol.* **2020**, *96*, 14−20.
(25) Kutsumura, N.; Kiriseko, A.; Saito, T. Total Synthesis of (+)-Heteroplexisolide E. *Heterocycles* **2012**, *86*, 1367−1378.
(26) Cravatt, B. F.; Wright, A. T.; Kozarich, J. W. Activity-based protein profiling: From enzyme chemistry. *Annu. Rev. Biochem.* **2008**, *77*, 383−414.
(27) Speers, A. E.; Adam, G. C.; Cravatt, B. F. Activity-based protein profiling in vivo using a copper(I)-catalyzed azide-alkyne [3 + 2] cycloaddition. *J. Am. Chem. Soc.* **2003**, *125*, 4686−4687.
(28) Widen, J. C.; Kempema, A. M.; Villalta, P. W.; Harki, D. A. Targeting NF-kappa B p65 with a Helenalin Inspired Bis-electrophile. *ACS Chem. Biol.* **2017**, *12*, 102−113.
(29) Hutchinson, E. C.; Orr, O. E.; Man Liu, S.; Engelhardt, O. G.; Fodor, E. Characterization of the interaction between the influenza A virus polymerase subunit PB1 and the host nuclear import factor Ran-binding protein 5. *J. Gen. Virol.* **2011**, *92*, 1859−1869.
(30) Levin, A.; Neufeldt, C. J.; Pang, D.; Wilson, K.; Loewen-Dobler, D.; Joyce, M. A.; Wozniak, R. W.; Tyrrell, D. L. J. Functional Characterization of Nuclear Localization and Export Signals in Hepatitis C Virus Proteins and Their Role in the Membranous Web. *PLoS One* **2014**, *9*, e114629.
(31) Zhang, W. J.; Lu, Y. X.; Li, X. M.; Zhang, J. M.; Lin, W. H.; Zhang, W.; Zheng, L.; Li, X. N. IPO5 promotes the proliferation and tumourigenicity of colorectal cancer cells by mediating RASAL2 nuclear transportation. *J. Exp. Clin. Cancer Res.* **2019**, *38*, 296.
(32) Harmange Magnani, C. S.; Thach, D. Q.; Haelsig, K. T.; Maimone, T. J. Syntheses of Complex Terpenes from Simple Polyprenyl Precursors. *Acc. Chem. Res.* **2020**, *53*, 949−961.
(33) Chen, D. Z.; Evans, P. A. A Concise, Efficient and Scalable Total Synthesis of Thapsigargin and Nortrilobolide from (R)-(−)-Carvone. *J. Am. Chem. Soc.* **2017**, *139*, 6046−6049.
(34) Chu, H.; Smith, J. M.; Felding, J.; Baran, P. S. Scalable Synthesis of (−)-Thapsigargin. *ACS Cent. Sci.* **2017**, *3*, 47−51.
(35) Siemon, T.; Wang, Z. Q.; Bian, G. K.; Seitz, T.; Ye, Z. L.; Lu, Y.; Cheng, S.; Ding, Y. K.; Huang, Y. L.; Deng, Z. X.; et al. Semisynthesis of Plant-Derived Englerin A Enabled by Microbe Engineering of Guaia-6,10(14)-diene as Building Block. *J. Am. Chem. Soc.* **2020**, *142*, 2760−2765.
(36) Li, X. F.; Aierken, A. L. D.; Shen, L. IPO5 promotes malignant progression of esophageal cancer through activating MMP7. *Eur. Rev. Med. Pharmaco.* **2020**, *24*, 4246−4254.
(37) Gorlich, D.; Kutay, U. Transport between the cell nucleus and the cytoplasm. *Annu. Rev. Cell Dev. Biol.* **1999**, *15*, 607−660.
(38) Mahipal, A.; Malafa, M. Importins and exportins as therapeutic targets in cancer. *Pharmacol. Ther.* **2016**, *164*, 135−143.
(39) Kosyna, F. K.; Depping, R. Controlling the Gatekeeper: Therapeutic Targeting of Nuclear Transport. *Cells* **2018**, *7*, 221.
(40) Fukuda, M.; Asano, S.; Nakamura, T.; Adachi, M.; Yoshida, M.; Yanagida, M.; Nishida, E. CRM1 is responsible for intracellular transport mediated by the nuclear export signal. *Nature* **1997**, *390*, 308−311.
(41) Kudo, N.; Matsumori, N.; Taoka, H.; Fujiwara, D.; Schreiner, E. P.; Wolff, B.; Yoshida, M.; Horinouchi, S. Leptomycin B inactivates CRM1/exportin 1 by covalent modification at a cysteine residue in the central conserved region. *Proc. Natl. Acad. Sci. U. S. A.* **1999**, *96*, 9112−9117.
(42) Gravina, G. L.; Senapedis, W.; McCauley, D.; Baloglu, E.; Shacham, S.; Festuccia, C. Nucleo-cytoplasmic transport as a therapeutic target of cancer. *J. Hematol. Oncol.* **2014**, *7*, 85.
(43) Wagstaff, K. M.; Sivakumaran, H.; Heaton, S. M.; Harrich, D.; Jans, D. A. Ivermectin is a specific inhibitor of importin alpha/beta-mediated nuclear import able to inhibit replication of HIV-1 and dengue virus. *Biochem. J.* **2012**, *443*, 851−856.
(44) Caly, L.; Druce, J. D.; Catton, M. G.; Jans, D. A.; Wagstaff, K. M. The FDA-approved drug ivermectin inhibits the replication of SARS-CoV-2 in vitro. *Antiviral Res.* **2020**, *178*, 104787.
(45) Deng, T.; Engelhardt, O. G.; Thomas, B.; Akoulitchev, A. V.; Brownlee, G. G.; Fodor, E. Role of ran binding protein 5 in nuclear import and assembly of the influenza virus RNA polymerase complex. *J. Virol.* **2006**, *80*, 11911−11919.
(46) Swale, C.; Da Costa, B.; Sedano, L.; Garzoni, F.; McCarthy, A. A.; Berger, I.; Bieniossek, C.; Ruigrok, R. W. H.; Delmas, B.; Crepin, T. X-ray Structure of the Human Karyopherin RanBP5, an Essential Factor for Influenza Polymerase Nuclear Trafficking. *J. Mol. Biol.* **2020**, *432*, 3353−3359.

https://doi.org/10.1021/acscentsci.1c00056
ACS Cent. Sci. 2021, 7, 954−962